Non – invasive Fetal Scalp pH Measurement Utilizing Magnetic Induction Spectroscopy Technique

Shazwani Sarkawi, Zulkarnay Zakaria, Ibrahim Balkhis, Jurimah Abd Jalil
Biomedical Electronic Engineering
School of Mechatronic
Universiti Malaysia Perlis
Arau, Perlis, Malaysia
shazwani.unimap@gmail.com

***Abstract*— Conventional fetal of fetal scalp sampling needs an invasive method to acquire blood sample to the fetus. In this paper describes a suggested non-invasive technique employing magnetic induction spectroscopy based on hydrogen conductivity in pH solution. Four types of transmitter-receiver (Tx-Rx) coil pairs are developed and test with frequency range from 2MHz to 10MHz. The phase reading from both reference channel, and sample channel is taken and the phase change is calculated from the differences between both channels. The result shows that the phase is decreased as the pH value of the solution increase. Circular pair of Tx-Rx shows a good sensitivity reading while square pair Tx-Rx shows a linearity result. From the result obtained, it is proved that single channel magnetic induction spectroscopy can be used as a non-invasive pH meter as an alternative to invasive pH meter.**

Index Terms– Fetal Scalp Sampling; Magnetic Induction Spectroscopy; Receiver; Transmitter.

I. INTRODUCTION

pH is a degree of acidity or alkalinity of the solution. This pH value is limited by the value of hydrogen or hydroxyl ions presents. Acid solution consists of higher relative number hydrogen ions, while alkaline or basic solution consists of higher relative number of hydroxyl ions [1], [2]. The retention of the hydrogen and hydroxyl can vary over 15 orders of magnitude in water. Henderson-Hasselbalch equation is used to describe the derivation of pH as a quantity of acid. This derivation is applicable in biological and chemical system which employing pKa, the negative log of the acid dissociation constant. Besides that, the equation is also beneficial for estimating the pH of buffer solution and getting the equilibrium pH in acid-base reaction. In blood pH, the Henderson–Hasselbalch equation can be used to relate the pH of blood to constituents of the bicarbonate buffering system [3]. The normal value of the pH is slightly basic which 7.25 [4]. This value is often brought up to as physiological pH in biology and medicine.

A.Fetal Scalp Sampling

Fetal hypoxia or intrauterine hypoxia is the condition occurs where the fetus is deprived an insufficient oxygen [5]. Fetal scalp blood sampling is one of the techniques that used to detect this fetal hypoxia. This procedure performed when is in active labor to determine whether the baby is getting enough oxygen [6]. The purposes of this testing are to prevent unnecessary intervention by investigation of pH and lactate values of fetal blood when there is suspicion of fetal compromises. Fetal scalp testing is a common test used before the mother giving birth to determine the oxygen level of the baby through blood pH. This test is important because it will determine whether the fetal is ready to be delivered as well as to find the most suitable technique to deliver the baby, either normal birth or caesarean [7], [8]. Conventional technique for this test requires the doctor to slice the fetal scalp a bit using forceps and draw the blood from there [4]. The blood then taken to the lab for analysis, which consuming times [9]. This method may lead to continuing bleeding in fetal scalp and swollen, which is very dangerous to the fetal, besides arise trauma to the mother. Besides that, the analysis of pH requires a relatively large amount of blood (30-50 µl), and sampling failure rates of 11-20% have been reported [10]. Thus, non-invasive technique is proposed as an alternative to this fetal conventional method.

B.Magnetic Induction Spectroscopy

For the non-invasive technique, single magnetic induction setup (MIS) is suggested as the best way to detect low conductivity of biological tissues. This is because MIS is sensitive to all biological tissue properties (conductivity, permittivity, permeability), however, conductivity is always considered as it is the dominant compared to other properties [11], [12]. This single channel spectroscopy consists of one transmitter and one receiver. The AC signal is supply to the transmitter and generate primary field. After the fields penetrate into the object with conductivity, eddy current will induced. These eddy current depends on object dielectric which in this case, conductivity. The object will produce secondary field, which weakens the original primary field, due to Lenz' Law [13]. This secondary field will receive by the receiver [14]. The eddy current produced because of the Faraday's Law of Induction, where time-varying magnetic field, H induces an electrical field E.

Study of electromagnetic field will involve with Maxwell's equation. The Maxwell's equation is:

$$V\nabla \times \boldsymbol{E} = -j\omega \boldsymbol{B} \quad (1)$$

$$\nabla \times \boldsymbol{H} = (\sigma + j\omega\varepsilon)\boldsymbol{E} \quad (2)$$

$$\nabla \cdot \boldsymbol{D} = \rho \quad (3)$$

$$\nabla \cdot \boldsymbol{B} = 0 \quad (4)$$

From that equation, when electromagnetic is penetrating a sample, induced eddy current are created by the material itself. This occurs because of electrical properties of the sample is passive [15]. We can use Biot-Savart law to calculate the strength of the magnetic field from any areas in the ROI when induced eddy current are created. The equation of Bio-Savart law is:

$$\boldsymbol{B} = \mu_0 \sum_V \frac{JdV \times \rho}{4\pi\rho^3} \quad (5)$$

Based on the equation above, we should know that the magnitude of the field strength of magnetic, B is relies on the volume and also the area covered by the field dV [16]. The formula below show how frequency depends on the field is penetrating inside the samples which are:

$$d = \frac{1}{\omega}\sqrt{\frac{2}{\mu\varepsilon_0\varepsilon_r \tan\delta}} \quad (6)$$

Thus equation represent which is *d* is penetration depth, ω is frequency, μ is permeability, ε_0 is free space permittivity,ε_r is relative permittivity and tan δ is loss factor [15]. Thus, this how Maxwell equation is expanding on the concept of the magnetic field.

Numerous researches concentrate on using different methods to simulate the interaction between matter and radiated energy, however the Magnetic Induction Spectroscopy (MIS) is preferred as it eliminates some difficulties of fully non- contacting inductive coupling between the sensor and the sample or in this case biological tissue [17]. Funk et *al* [18] found that magnetic field can penetrate cells more deeply than electric field, as the cell membranes high dielectric property has a shielding effect. It also can influence chemical and biochemical reactions because human body is 'semitransparent' to magnetic field [19]. Hevia – Montiel et *al* applied MIS Setup to detect early breast cancer. They suggested that the utilization of tissue bioimpedance estimations by multiple frequency magnetic fields as a valuable alternative to detect non-invasively breast neoplasm and MIS was used to measure the electrical properties of tissue at different frequencies [20].

Simulation of multi-frequency induced current was done by Cesar et *al* [21]. Their aim was to assess analytically and experimentally the inductive phase shift as a function of multi-frequency induced in breast cancer condition. The magnetic induction method was used to anticipate the inductive phase shift as a function of the bulk electrical properties in typical breast volumes with tumors in particular positions.

C. Phase Shift Measurement

The phase shift or phase angle is the time relationship of two periodic signals of the same frequency. Phase measurement is a process of defining the phase deviation between two periodic signals, the input signal and the reference signal.

Phase detector is a device that used to detect or measure the phase difference between two input signals. To measure the phase in digital technique, the two input signals are converted into a square form. In fact, there are various phase measurement methodologies applied in measuring phase shifts or phase angles in the magnetic induction spectroscopy system. In magnetic induction setup, these two field are sensed by a receiving coil, and the phase shift between the exciting field and the superimposed field is proportional to the conductor of the object and signal frequency [22]. The phase shift usually measured by phase measurement hardware. The most common phase measurement hardware that uses in magnetic induction is lock-in amplifier [23]–[25].

Deng et *al* [26] studies on the phase shift method to measure the blood perfusion of biological tissues. The dual reciprocity boundary element method (DRBEM) was applied to numerically solve the transient and non-linear two-dimensional bio-heat transfer in biological bodies subject to a sinusoidal heat flux at the skin surface.

Rojas et *al* [27] proposed a numerical simulation technique to detect a phase shift through measurement of induced electrical currents due to a radio frequency signal of brain edema. Phase shift shows sensitivity to the presence of the edema or hemotoma increased with frequency.

The development of non-invasive optical polarimetric glucose sensing Cotc et *al* [28]. This prototype utilizes a true phase measurement technique in order to monitor in vivo glucose concentration. The helium neon laser light was applied which coupled through a rotating linear polarizer along with two stationary linear polarizers and two detectors to produce reference and signal outputs whose amplitudes varied sinusoidally with a frequency of twice the angular velocity of the rotating polarizer, and whose phase was proportional to the rotation of the linear polarization vector passing through the glucose solution.

II. METHODOLOGY

A.Hardware Development

The MIS system is mainly consists of three sub-system which are the sensor jig, signal conditioning circuit and the host computer.

Four pairs of transmitter and receiver coil had been developing. The design includes two types of transmitter coil and four types of receiver coil had been developed and had been fabricated on the PCB board. There are two types of pair which is square coil and circular coil pair. The coil specification of transmitter was shown in Table 1 while the coil specification for receiver shown in Table 2.

Table 1
Design specification of transmitter design

Properties	Circular Coil	Square Coil
Outer diameter	5.0 cm	5.0 cm
Inner diameter	4.0 cm	4.0 cm
Number of turns	5 turns	5 turns

The data will transfer to the PIC for preprocessing and display in the laptop. Visual Basic C# is used to develop the Graphical User Interface (GUI).

Table 2
Design specification of receiver design

Properties	Circular Pair 1	Circular Coil 2	Square Coil 1	Square Coil 2
Outer diameter	6.0 cm	6.0 cm	6.0 cm	6.0 cm
Inner diameter	5.2 cm	4.8 cm	5.2cm	4.8 cm
Number of turns	8 turns	12 turns	8 turns	12 turns

B.Hardware Setup

The transmitter and receiver coil was placed facing vertically to each other. Then, the transmitter coil was connected to the excitation circuit and Channel A from the frequency source, while the receiver coil was connected to detection circuit and Channel B from the frequency source. Typically, the excitation circuit excites the transmitter coil and the generated primary field. According to the mutual inductance technique, an eddy current is induced in the region of interest generate the secondary field. The eddy current produced was depending on the conductivity of the object [29]. The field will detect by the receiver coil with the help of receiver circuit. The range of frequency used is in MegaHertz (MHz). This frequency is choosing to increase the induced or secondary field. This is because the biological tissue has a very small conductivity value ($\sigma < 3$ Sm^{-1}) [22], [30]. The phase detector used in this experiment is AD8302. This is because AD8302 is a fully integrated RF IC for measuring differences in phase between two signals with a resolution of 10 mV/degree [31].

C. Experimental Procedure

pH solution from the range 7.20 – 7.40 was prepared as the solution of interest. Interest solution is placed on the sensor jig for 2 minutes. 2 minutes is choosing to give capacitor in the phase detector some times to charge and discharge. The phase reading will show in the GUI.

The MIS system needs to be connected to the 5V of power supply and also power generator. The power generator was set up to 1V peak-to peak/VPP. The phase detector will send the phase shift through wireless to the computer by 2.4 GHz XBee XB24-Z7WIT-004 modules. The output of the system or the phase shift will be display on graphical user interfaces (GUI) as a phase shift display. The GUI will calculate the mean, standard deviation, mode and median of the output data. The time setting to obtain the data is set to 120 seconds per data input. Thus each solution will be measured about 2 minutes; additional 2 minutes will be measured without solution for reference purpose.

III. Result And Discusion

The data collection will consist set of data with 4 pair coil that had been develop before, the first pair is circular pair of with 5 turn Tx and 8 turn of Rx coil followed by second circular pair with 5 turn Tx and 12 Rx coil and then the third is square pair with 5 turn Tx and 8 turn Rx coil. Last pair is square pair with 5 turn Tx and 12 turn Rx coil. The 5 sample of different pH value (7.20, 7.25, 7.30, 7.35, and 7.40) are tested on every pair coil sensor. Each pair are tested with 5 different frequency of 2MHz, 4MHz, 6MHz, 8MHz and 10MHz which set up in the power generator.

The result obtained was observed and arranged all the data in the Microsoft Excel according to the 4 pairing coil with different frequency. The phase change calculated by the difference between the references of output with the mean of phase output for every frequency from 2MHz to 10 MHz. Table 3 shows the result of phase change for circular pair of coil with 5 turns for transmitter and 8 turns for the receiver. The data in the table show that phase shift value is negative value which this shows that magnetic field produce in the receiver is negative. Thus, this due to the secondary field generated by the receiver coil opposed the direction of the primary field. The value of phase changes decreases for every increment of frequency and phase change, decreasing inversely proportional to the pH value when increase. The value in Table 3 then plotted in graphical form as shown in Figure 1.

Table 3
Phase change of 5Tx-8Rx pair

pH Value	2MHz	4MHz	6MHz	8MHz	10MHz
7.20	-0.098	-0.279	-0.410	-0.346	-0.590
7.25	-0.248	-0.160	-0.438	-0.570	-0.858
7.30	-0.193	-0.208	-0.636	-0.853	-1.049
7.35	-0.209	-0.412	-0.894	-1.147	-1.618
7.40	-0.250	-0.571	-0.916	-1.334	-1.619

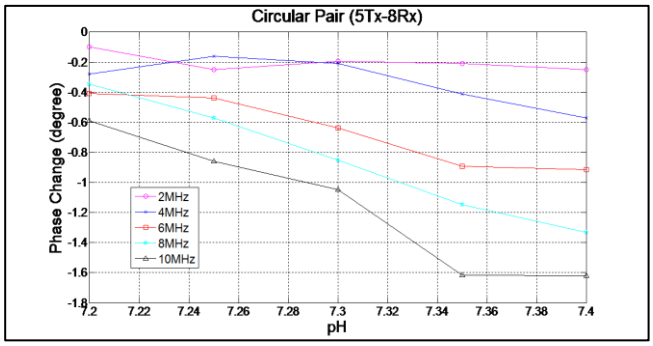

Figure 1**:** Result of phase change for Circular Pair (5Tx-8Rx)

Figure 1 shows that from 6 MHz to 10 MHz, the phase shift values are gradually decreased against the increment of pH value. In other hand, at 2 MHz show an increment at pH value of 7.30 with -0.193 degree of phase shift. n the same time, at 4 MHz also show some increment at 7.25 and 7.30 pH values with -0.160 and -0.208 degree phase shift. From the result, frequency of 10 MHz shows a huge different phase shift between each frequency. In addition, at 8 MHz show a linearity of decreasing phase shift along the increment of pH value applied.

Thus, the graph of phase shift against the pH value is plotter by using MATLAB software for all 4 pair. The graphs are as shown in the Figure 2-4 for each pair.

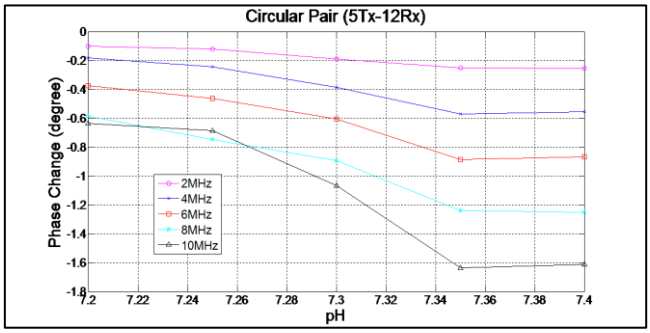

Figure 2: Result of phase change for Circular Pair (5Tx-12Rx)

The Figure 2 shows most of the frequency gives linearity decrement from 7.20 to 7.35 pH value and at 7.40, pH the value gently start to increase. At 10 MHz show shows suddenly drop of value at 7.25 pH value and continue a with a linearity decrement.

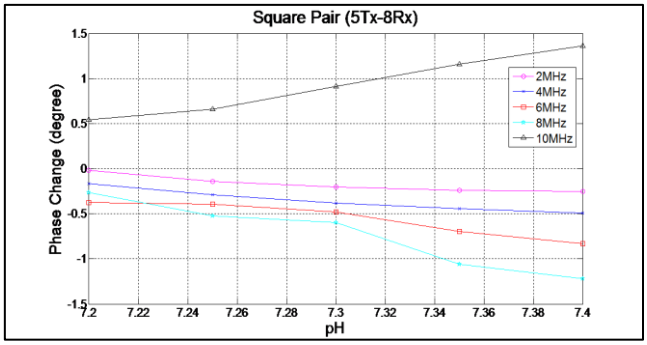

Figure 3. Result of phase change for square pair (5Tx-8Rx)

From Figure 3, from 2 MHz to 6 MHz show a steadily dropped and show linearity along the graph dropped. However, at 8 MHz show some fluctuated decrement of value from 7.25-7.35 of pH value. Then followed by 10 MHz, which inversely rose along the graph due to when setting up the power generator for 10 MHz, the phase reaches a maximum value of 180 degree. Thus the power generator needs to be set up inversely, which negative phase. This makes the 10 MHz are differ from other.

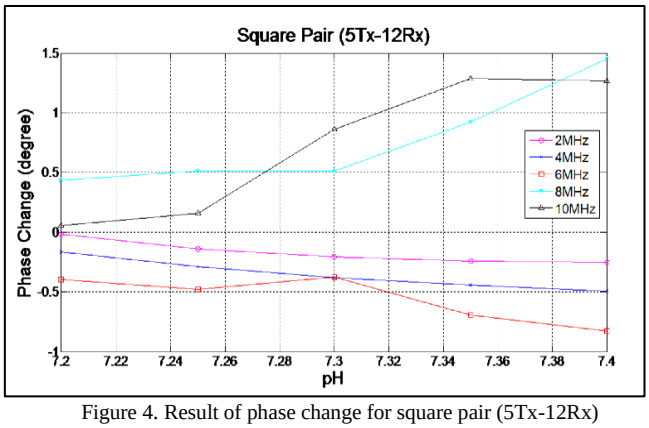

Figure 4. Result of phase change for square pair (5Tx-12Rx)

The Figure 4 point that from 2 MHz to 4 MHz gives a linear decrement along the graph and at 6 MHz there are slightly rose at 7.30 pH value. Differ from other frequency which 8 and 10 MHz give a steeply increment, which stated in the paragraph before that the power generator need to be set up a negative value of phase. This pair shows that it is not suitable to be used in the MIS system due to unstable increment or decrement of phase shift, although it show a linearity decrement but the phase difference between pH values are too small.

From the result, it shows that phase change decreasing as the value of pH increase. This is because the greater the conductivity changes, the greater the phase shift generated [32]. According to A. Kapus et *al* [33], a positive values indicate relative internal acidity, thus this stated that the increasing value of pH will lead to drop down of the voltage. As back to basic which the concentration of the pH depends on the hydrogen ion. The more hydrogen ion were added the less pH value will be and became acidic. The conductivity is the measure concentration of all active ions in the solution. Thus to relate the conductivity to the pH value is based on what is what the major concentration that are to calculate. The conductivity of the solution can be inversely proportional to the value of pH when consider the OH+ as the main major factor to measures.

By taking only 10MHz result for each pair, the phase then converts into voltage by using formula of:

$$V_{out} = \frac{G - 90}{0.01} \tag{7}$$

Where, the value of V_{out} is the voltage output is calculated by the subtraction of the phase shift, G with 90 degree of shift. Then the value will be divided by attenuation of 0.01. 10 MHz is chosen as the best frequency because the whole system measurement system requires a phase measurement accuracy least 0.01° when frequency of the exciting signal is 10MHz, [34]. Linear regression for each pair is then plotted to show the relationship between the voltage and pH value. The result was plotted by MATLAB and the graphs are shown in Figure 5-9.

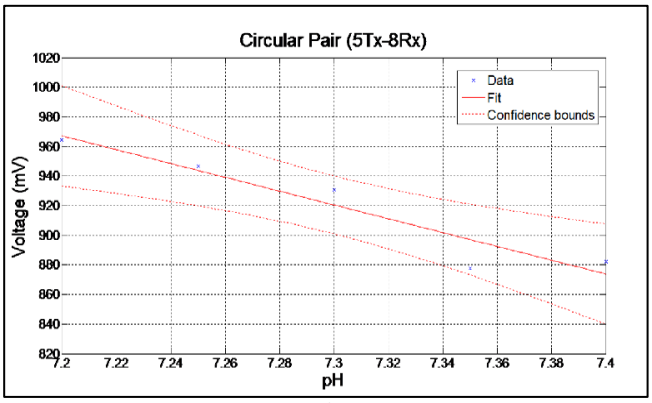

Figure 5. Linear regression for circular coil pair (5Tx-8Rx)

The linear regression are based on the Voltage against the pH value with 10 MHz are applied to the system. Based on Figure 5, the developed equation determined as follow:

$$y_{predicted} = -466.8x + 4328.1 \tag{8}$$

$$R^2 = 0.9194 \tag{9}$$

Where y is the predicted degree of the phase change, x is the pH value of the solution and R^2 is coefficient of determination.

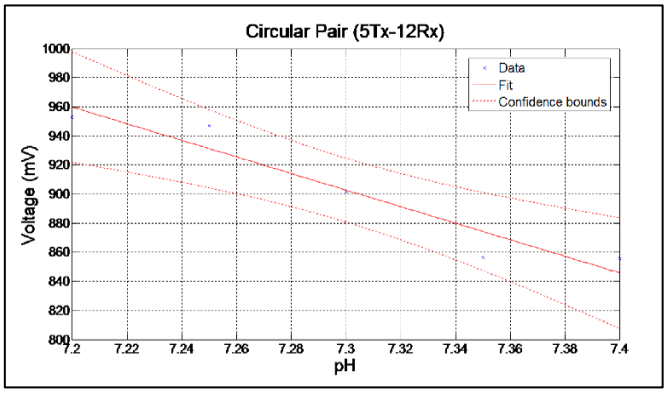

Figure 6. Linear regression for circular coil pair (5Tx-12Rx)

Next is the circular pair that consists with 5 turns for transmitter and 12 turns for receiver. Linear regression plotted as shown in Figure 6 and the developed equation is determined as follow:

$$y_{predicted} = -569.8x + 5062.2 \quad (10)$$

$$R^2 = 0.9058 \quad (11)$$

Where y is the predicted degree of the phase change, x is the pH value of the solution and R^2 is coefficient of determination. The Figure 7 show that linear regression plot for square pair with 5 turns in transmitter coil and 8 turns in receiver coil.

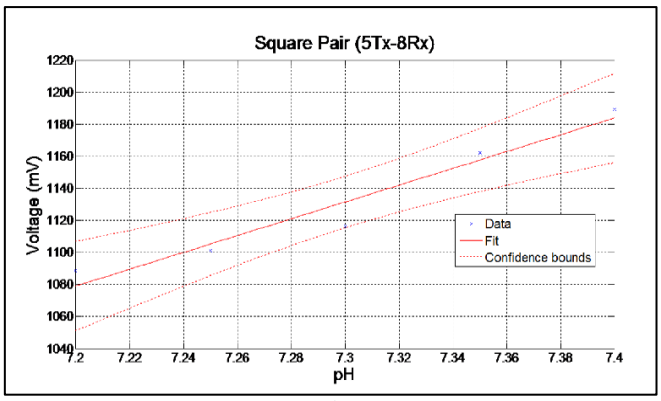

Figure 7. Linear regression for square coil pair (5Tx-8Rx)

The third equation that identified from Figure 7 as follow:

$$y_{predicted} = -524.4x - 2696.6 \quad (12)$$

$$R^2 = 0.9472 \quad (13)$$

Where y is the predicted degree of the phase change, R^2 is the coefficient of determination and x is the pH value of the solution. In Figure 7, clearly can be seen three values of the actual value are near to the predicted value, but the other 2 value are much different the distance between the real and the predicted data.

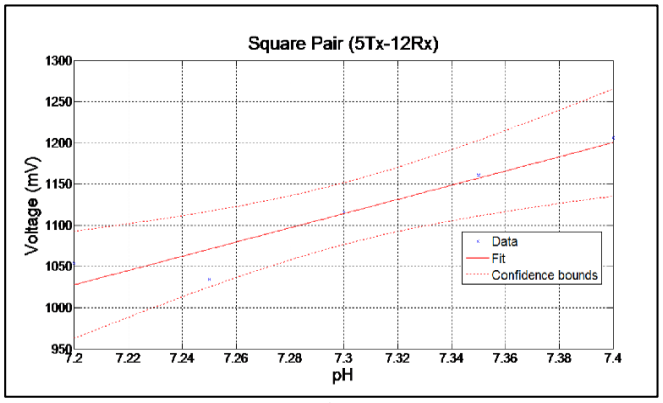

Figure 8. Linear regression for square coil pair (5Tx-12Rx)

Last but not least, the linear regression of square pair (5Tx-12Rx) is plotted as shown in Figure 8 and the equation is determined as follow:

$$y_{predicted} = -862.4x - 5181.3 \quad (14)$$

$$R^2 = 0.8991 \quad (15)$$

Where y is the predicted degree of the phase change, x is the pH value of the solution and R^2 is the coefficient of determination. In this Figure 9, all data are aligned near to the predicted value. The two results proved that the linearity of the square pair 1 and 2 are much more linear than the round pair. Thus, by determining all the best fit equation for each of the pairing coil, the relationship between produced voltages at the receiver over the pH value of the solution of interest through application of magnetic induction technique are determined. From this equation, any unknown pH value of a solution can be predicted based on voltage.

In other hand, from those 4 pairs the Figure show that the circular shape proved the increasing of pH will lead to decreasing of the voltage output. Thus, this proves that voltage is inversely proportional to the pH. Besides that, both square pairs show an increment of voltage when the pH value are increasing. This is due to changes in phase direction which is negative phase in power generator when using a square pair. The limit for generator is 180 phase, but square coil pair need a higher degree of phase. Then square coil pair still acceptable and proved that there are relation between pH and the voltage. In other hand, the orientation of the coil is one of the factors that change the phase to become negative value.

Circular type is chosen as the best transmitter and receiver coil because it has a higher sensitivity value [35]. As the result, the graph shows large different bending on each point of pH value. According to Norhisam Nisron et *al* [35] result show that circle coil will give more sensitivity performance but inversely it will give low linearity.

IV. CONCLUSION

In conclusion, it proves that the MIS setup can be used to analyses a different hydrogen conductivity of pH solution. The final result shows the capability of the system to detect a small and large pH value. So, this system is applicable to use in detecting the pH value of fetal scalp blood non-invasively. The potential of this setup to detect smallest changes in the pH solution makes it an excellent non-invasive technique to detect blood pH within 7.20-7.40.

Circular type of transmitter and receiver coil is preferred as it is more sensitive. The range of frequency must be higher to increase the capability of eddy current induced. Basically the system is easy to design and much cheaper compared to other current image tomography devices. For future works, the resolution of this MIS setup can be increased to make the setup more accurate.

REFERENCES

[1] M. G. Abdullah, M. C. Anderson, M. J. Anderson, A. Augustyn, and M. L. Barton, "pH," *Britannica Online Encyclopedia*. pp. 1–2, 2014.

[2] M. Filomena Camoes, "A Century of pH Measurement," *Chemistry International*, vol. 32, no. 2, pp. 3–7, Mar-2010.

[3] R. W. Burnett and D. C. Noonan, "Calculations and Correction Factors Used in Determination of Blood pH and Blood Gases," *Clin. Chem.*, vol. 20, no. 12, pp. 1499–1506, 1974.

[4] Women and Newborn Health Service, "Fetal scalp blood sampling," in *Clinical Guidelines*, King Edward Memorial Hospital, 2008, pp. 1–4.

[5] G. Kendall and D. Peebles, "Acute fetal hypoxia: The modulating effect of infection," *Early Hum. Dev.*, vol. 81, no. 1, pp. 27–34, 2005.

[6] N. K. Kaneshiro and D. Zieve, "Fetal scalp pH testing," *MedlinePlus Medical Encyclopedia*, vol. 1, no. 1. U.S National Library of Medicine, pp. 1–2, 2012.

[7] M. Holzmann, S. Wretler, S. Cnattingius, and L. Nordström, "Neonatal outcome and delivery mode in labors with repetitive fetal scalp blood sampling," *Eur. J. Obstet. Gynecol. Reprod. Biol.*, vol. 184, pp. 97–102, 2015.

[8] J. S. Jørgensen and T. Weber, "Fetal scalp blood sampling in labor - A review," *Acta Obstet. Gynecol. Scand.*, vol. 93, pp. 548–555, 2014.

[9] D. Tuffnell, W. L. Haw, and K. Wilkinson, "How long does a fetal scalp blood sample take?," *BJOG An Int. J. Obstet. Gynaecol.*, vol. 113, pp. 332–334, 2006.

[10] E. Wiberg-Itzel, C. Lipponer, M. Norman, A. Herbst, D. Prebensen, A. Hansson, A.-L. Bryngelsson, M. Christoffersson, M. Sennström, U.-B. Wennerholm, and L. Nordström, "Determination of pH or lactate in fetal scalp blood in management of intrapartum fetal distress: randomised controlled multicentre trial.," *BMJ*, vol. 336, no. 1, pp. 1284–1287, 2008.

[11] Z. Zakaria, N. Aqma, H. Mohd, N. H. Jaafar, M. F. Jumaah, S. B. Mansor, and R. A. Rahim, "Initial Results on Magnetic Induction Tomography Hardware Measurement Using Hall Effect Sensor Application," *IEEE EMBS Conf. Biomed. Eng. Sci. (IECBES 2010)*, vol. 1, no. 1, pp. 9–12, 2010.

[12] Z. Zakaria, R. Abdul Rahim, M. S. B. Mansor, S. Yaacob, N. M. N. Ayub, S. Z. M. Muji, M. H. F. Rahiman, and S. M. K. S. Aman, "Advancements in transmitters and sensors for biological tissue imaging in magnetic induction tomography.," *Sensors (Basel).*, vol. 12, no. 6, pp. 7126–56, Jan. 2012.

[13] C. H. Riedel and O. Dossel, "Non-contact measurement of the electrical impedance of biological tissue," *2001 Conf. Proc. 23rd Annu. Int. Conf. IEEE Eng. Med. Biol. Soc.*, vol. 3, pp. 3077–3080, 2001.

[14] H. Scharfetter, R. Casañas, and J. Rosell, "Biological Tissue Characterization by Magnetic Induction Spectroscopy (MIS): Requirements and Limitations," *IEEE Trans. Biomed. Eng.*, vol. 50, no. 7, pp. 870–880, 2003.

[15] Z. Zakaria, N. Z. M. Alia, R. A. Rahim, M. S. Badri, and A. D. M. Rahim, "Simulation of Electromagnetic Field (EM) Focusing Capability on Biological Tissue through the Application of C-type Excitation Coil Screen," in *2012 International Conference on Biomedical Engineering (ICoBE)*, 2012, vol. 1, pp. 598–601.

[16] A. Barai, S. Watson, H. Griffiths, and R. Patz, "Magnetic induction spectroscopy: non-contact measurement of the electrical conductivity spectra of biological samples," *Meas. Sci. Technol.*, vol. 23, no. 8, pp. 1–11, Aug. 2012.

[17] C. A. González, M. Pérez, N. Hevia, F. Arámbula, O. Flores, E. Aguilar, I. Hinojosa, L. Joskowicz, and B. Rubinsky, "Over-hydration detection in brain by magnetic induction spectroscopy," *J. Phys. Conf. Ser.*, vol. 224, pp. 1–4, 2010.

[18] R. H. W. Funk, T. Monsees, and N. Özkucur, "Electromagnetic effects - From cell biology to medicine," *Prog. Histochem. Cytochem.*, vol. 43, no. 4, pp. 177–264, 2009.

[19] M. Cifra, J. Z. Fields, and A. Farhadi, "Electromagnetic cellular interactions," *Prog. Biophys. Mol. Biol.*, vol. 105, no. 3, pp. 223–246, 2011.

[20] N. Hevia-Montiel, E. S. Soto, and C. A. Gonzalez-diaz, "Early Breast Cancer Detection by Magnetic Induction Spectroscopy," *Transcations Japanese Soc. Med. Biol. Eng.*, vol. 33, no. 2, p. 2012, 2012.

[21] C. A. González, "Simulation of Multi-Frequency Induced Currents in Biophysical Models and Agar Phantoms of Breast Cancer," *J. Electromagn. Anal. Appl.*, vol. 4, no. 1, pp. 317–325, 2012.

[22] G. Jin, J. Sun, M. Qin, Chao Wang, W. Guo, Q. Yan, B. Peng, and W. Pan, "A Special Phase Detector for Magnetic Inductive Measurement of Cerebral Hemorrhage," *PLoS One*, vol. 9, no. 5, pp. 1–7, 2014.

[23] W. He, H. Luo, Z. Xu, and J. Wang, "Multi-channel magnetic induction tomography measurement system," *Proc. - 2010 3rd Int. Conf. Biomed. Eng. Informatics, BMEI 2010*, vol. 1, pp. 402–405, 2010.

[24] C. H. Igney, R. Pinter, A. Brauers, O. Such, and M. S. Processing, "Planar magnetic induction impedance measurement system with normal sensor alignment for vital signs detection," vol. 1. pp. 8–11, 2005.

[25] S. Watson, R. J. Williams, W. Gough, and H. Griffiths, "A magnetic induction tomography system for samples with conductivities below 10 S m−1," *Meas. Sci. Technol.*, vol. 19, no. 1, pp. 1–11, 2008.

[26] Z. S. Deng and J. Liu, "Parametric studies on the phase shift method to measure the blood perfusion of biological bodies.," *Med. Eng. Phys.*, vol. 22, no. 10, pp. 693–702, Dec. 2000.

[27] R. Rojas and A. O. Rodriguez, "Numerical Simulation of Inductive Phase Shift Due a Brain Hematoma," *PIERS Online*, vol. 6, no. 7, pp. 646–650, 2010.

[28] G. L. Cotc, M. D. Fox, and R. B. Northrop, "Noninvasive Optical Polarimetric Glucose Sensing Using a True Phase Measurement Technique," *IEEE Trans. Biomed. Eng.*, vol. 39, no. 7, pp. 752–756, 1992.

[29] S. Zlochiver, "Induced Current Electrical Impedance Tomography for Medical Applications," Tel Aviv University, 2005.

[30] Z. Zakaria, L. P. Yern, A. Azamimi, R. A. Rahim, and M. S. Badri, "Simulation Study on Size and Location Identification of Tumors in Liver Tissue through Eddy Current Distribution Analysis," *Int. Conf. Biomed. Eng.*, vol. 1, no. 1, pp. 602–604, 2012.

[31] C. A. Gonzalez, J. A. Valencia, A. Mora, F. Gonzalez, B. Velasco, M. A. Porras, J. Salgado, S. M. Polo, N. Hevia-Montiel, S. Cordero, and B. Rubinsky, "Volumetric Electromagnetic Phase-Shift Spectroscopy of Brain Edema and Hematoma," *PLoS One*, vol. 8, no. 5, pp. 1–10, 2013.

[32] W. Pan, Q. Yan, M. Qin, G. Jin, J. Sun, X. Ning, W. Zhuang, B. Peng, and G. Li, "Detection of Cerebral Hemorrhage in Rabbits by Time-Difference Magnetic Inductive Phase Shift Spectroscopy," *PLoS One*, vol. 10, no. 5, pp. 1–14, 2015.

[33] A. Kapus, R. Romanek, and A. Yi, "A pH-sensitive and Voltage-dependent Proton Conductance in the Plasma Membrane of Macrophages," vol. 102, no. October, pp. 729–760, 1993.

[34] S. Watson, R. J. Williams, H. Griffiths, W. Gough, and A. Morris, "A Transceiver For Direct Phase Measurement Magnetic Induction Tomography," *Proc. 23rd Annu. EMBS Int. Conf.*, vol. 4, pp. 3–6, 2001.

[35] N. Misron, L. Q. Ying, R. N. Firdaus, N. Abdullah, N. F. Mailah, and H. Wakiwaka, "Effect of inductive coil shape on sensing performance of linear displacement sensor using thin inductive coil and pattern guide," *Sensors*, vol. 11, no. 11, pp. 10522–10533, 2011.